MAUSAM, **65**, 4 (October 2014), 461-480

551.528.8 : 551.577.21

Impact study of integrated precipitable water estimated from Indian GPS measurements

SURYA K. DUTTA, V. S. PRASAD and D. RAJAN

National Centre for Medium Range Weather Forecasting, Noida – 201 307, U. P., India

(*Received 4 September 2012, Modified 1 August 2013*)

e mail : vsprasad@ncmrwf.gov.in

सार – इस शोध पत्र में ग्लोबल पोजिशनिंग सिस्टम एवं भारतीय मौसम स्टेशनों नामत: चेन्नै, गुवाहटी, कोलकाता, मुम्बई और नई दिल्ली से प्राप्त किए गए समेकित वर्षणीय जल (आई.पी.डब्ल्यू.) आंकड़ों को राष्ट्रीय मध्य अवधि मौसम पूर्वानुमान (एन. सी. एम. आर. डब्ल्यू. एफ.) के ग्लोबल डेटा एसिमिलेशन प्रणाली (जी. डी. ए. एस.) में सम्मिलित करके अध्ययन किया गया है। जी. डी. ए. एस. विश्लेषण के ग्रिड प्वाइंट सांख्यिकीय अंतर्वेशन (जी. एस. आई.) योजना का ग्लोबल मॉडल टी254एल64 के साथ प्रयोग किया गया है। वेव संख्या 254 का 64 स्तरों की उँचाई पर त्रिभुजाकार विकृति में विश्लेषण किया गया है और पूर्वानुमान दिया गया है। आवर्ती समय योजना के अनुसार प्रतिदिन चार बार (0000 यू. टी. सी., 0600 यू. टी. सी., 1200 यू. टी. सी. और 1800 यू. टी. सी. पर) ग्लोबल विश्लेषण किया गया है। लगभग 168 घंटों तक मॉडल के संयोजन किए गए है। इस शोध पत्र में पाया गया है कि विभिन्न मौसम विज्ञानिक प्राचलों के ऊपर समेकित वर्षणीय जल का प्रभाव पड़ा है। इस अध्ययन से यह पता चला है कि समेकित वर्षणीय जल (आई. पी. डब्ल्यू.) आंकड़ों के सम्मिलन से विश्लेषण और वेदर मॉडल टी354एल64 से संबंधित पूर्वानुमान प्रभावित हुए हैं। यह उपर्युक्त पॉच भारतीय मौसम स्टेशनों के आई. पी. डब्ल्यू आंकड़ों का ग्लोबल मॉडल में सम्मिश्रण करने का प्रयास तथा भारतीय क्षेत्र में विभिन्न मौसम विज्ञानिक प्राचलों के ऊपर पड़ने वाले प्रभावों का परीक्षण मात्र है। ऐसा पाया गया है कि 750 हेक्टापास्कल दाब के ऊपर के स्तरों में क्षेत्रीय और दक्षिणी पवन के अवयवों का आई. पी. डब्ल्यू. विश्लेषण में बहुत कम झुकाव है। आई. पी. डब्ल्यू. अनुरूपण से दिए गए पूर्वानुमान लगातार 850 हेक्टापास्कल दाब पर पवन वेक्टर औसत वर्गमूल त्रुटि (आर. एम. एस. ई.) से कम पाई गई है जबकि 250 हेक्टापास्कल दाब पर आई. पी. डब्ल्यू. के द्वारा दिए गए पूर्वानुमानों में केवल प्रथम दिन और चौथै दिन के पूर्वानुमान में सुधार हुआ है तापमान के लिए 850 हेक्टापास्कल दाब पर आई. पी. डब्ल्यू. के पूर्वानुमान चौथे और पॉचवे दिन के लिए अधिक वैध है। 250 हेक्टापास्कल दाब पर आई. पी. डब्ल्यू. से दिए गए प्रथम दिन के पूर्वानुमानों में तापमान आर. एम. एस. त्रुटि कम है। 250 हेक्टापास्कल दाब पर आई. पी. डब्ल्यू. से दिए गए औसत त्रुटि सभी दिनों के पूर्वानुमानों से कम है। 250 हेक्टापास्कल दाब पर आई. पी. डब्ल्यू. से दिए गए पूर्वानुमानों की भू-विभव आर.एम.एस. त्रुटि भी सभी दिनों के पूर्वानुमानों से कम है। पूर्वानुमानों और विश्लेषणों के अध्ययन से विसंगति और पैटर्न सहसंबंधों पर आई. पी. डब्ल्यू. सम्मिलन के सकारात्मक प्रभाव का पता चलता है।

ABSTRACT. The Global Positioning System – Integrated Precipitable Water (IPW) data from Indian stations namely Chennai, Guwahati, Kolkata, Mumbai and New Delhi have been assimilated in the National Centre for Medium Range Weather Forecasting's (NCMRWF) Global Data Assimilation System (GDAS). Gridpoint Statistical Interpolation (GSI) Scheme of GDAS analysis is experimented with the global model T254L64. The analyses and forecasts are carried out at triangular truncation of wave number 254 and with 64 levels in vertical. Global analyses are carried four times (0000 UTC, 0600 UTC, 1200 UTC and 1800 UTC) daily with intermittent time scheme. Model integrations are carried up to 168 hours. The present study examines the impact that integrated precipitable water has over various meteorological parameters. The study reveals that the assimilation of IPW data influences the analyses and corresponding forecasts of the weather model T254L64. This is an attempt of assimilation of IPW data of the aforesaid five Indian stations in the global model and examination of corresponding impact on various meteorological parameters over Indian region. It is seen that for the layers above 750 hPa the zonal and meridional wind components for IPW analyses have less biases. Forecasts from IPW simulations are found to have consistently by lower 850 hPa wind vector root mean square error (RMSE) where as at 250 hPa, improvement in IPW runs are seen only for day-1 and day-4 forecasts. For temperature at 850 hPa, IPW forecasts valid for day-4 & day-5 are better. At 250 hPa, temperature RMSE for IPW runs is lower for day-1 forecasts. Mean error of IPW forecasts at 250 hPa is lower for all the days of forecasts. Also, geo-potential RMSE for the IPW runs at 250 hPa is lower for all the days of forecasts. Forecasts *vs* analyses study shows positive impact of IPW assimilation on the anomaly and pattern correlations.

Key words – IPW, GPS, Assimilation, GSI, GDAS, NWP, T254L64.

1. Introduction

Water vapour is one of the most significant constituents of the atmospheric composition, which plays a crucial role in the occurrence of weather systems and atmospheric phenomena over a wide range of spatial and temporal scales. It plays major role in atmospheric radiation and hydrological cycle. As the water's change of phase is associated with unusually large latent heat exchange with the atmosphere, the distribution of water vapour is important in the vertical stability of the atmosphere and is very intimately coupled with the distribution of clouds; hence, is important for accurate rainfall prediction. Water vapour moves rapidly through the atmosphere, redistributing energy through evaporation and condensation. This can vary abruptly over extremely short distances. For this reason, water vapour is under-observed in time and space.

2(a). *GPS IPW Data*

Integrated Precipitable Water (IPW) is the amount of atmospheric water vapour (in kilogram) overlying per unit area of the earth surface. Its unit is kg/m^2. The GPS (Global Positioning System) is a satellite based navigation system that consists of a network of 24 satellites placed into orbit in six orbital planes at an altitude of 20,200 km above the earth surface with an orbital period of 12 hrs. It transmits radio signals to a large number of users engaged in various fields including navigation, time transfer, and relative positioning (Leick, 1990). These GPS dual frequency L-band radio signals (L_1 = 1575 MHz; L_2 = 1225 MHz) are delayed by ionosphere and troposphere as they travel from GPS satellites to the ground based receivers. The ionosphere delay or error is rectified by the linear combination of L_1 and L_2 frequencies. But troposphere delay cannot be rectified easily. In the troposphere the GPS signals are delayed in part, by atmospheric water vapour generally referred to as zenith wet delay, (ZWD). Dry air, hydrometeors and other particulates are also responsible for the delay of the signals in reaching the ground based GPS receivers (Niell, 1996; Solheim *et al*., 1999) (referred to as zenith hydrostatic delay, ZHD). Since early 1990s various methods have been developed to use the wet delay data from GPS receivers to retrieve atmospheric column-integrated water vapour or precipitable water (PW) (Bevis *et al*., 1992, 1994; Rocken *et al*., 1993, 1997), ''slant water'' (Ware *et al*., 1997) and 3-dimensional (3-D) water vapour (MacDonald *et al*., 2002). The zenith wet delay (ZWD) at a radio receiver is nearly proportional to the precipitable water, that is, the vertically integrated water vapour overlying the receiver (Hogg *et al*., 1981; Askne and Nordius, 1987). This gives the possibility of using emerging networks of geodetic GPS receivers for remote sensing of atmospheric water vapour (Bevis *et al*., 1992; Rocken *et al*., 1993). GPS-sensed integrated precipitable water is found to have an accuracy (Root Mean Square Error) ranging from better than 2 mm in North America (Rocken *et al*., 1993, 1997; Duan *et al*., 1996; Fang *et al*., 1998) and Australia (Tregoning *et al*., 1998) to 2.2 mm in Taiwan (Liou *et al*., 2001) and 3.7 mm in Japan (Ohtani and Naito, 2000). These RMS errors are comparable to those of radiosonde and microwave radiometer measurements (Tregoning *et al*., 1998; Lijegren *et al*., 1999). Unlike microwave radiometers, however, GPS receivers work under all weather conditions. When compared with other measurements, the advantages of GPS-sensed integrated precipitable water include high sampling resolution (every few minutes or better), self-calibration, low cost and large coverage (Ware *et al*., 2000).

2(b). *Types of moisture measurements*

GPS-IPW is an indirect measurement of atmospheric water vapour. Some more techniques are also available for estimation of atmospheric water vapour using observations with space-based systems. Each one of them have their own inherent limitations. Those based on measurements of upwelling infrared radiation are reliable only in cloud free areas. Techniques based on measurement of upwelling microwave radiation (available only over oceans) are valid in cloudy regions, but are less accurate than the IR-based estimates. The GPS-IPW (Global-Positioning System - Integrated Precipitable Water) network makes it possible to make observations of IPW with high horizontal resolution (provided the ground network is dense enough), high temporal resolution, high accuracy, long-term measurement stability, and high reliability under all weather conditions. This GPS-based IPW measurement is most valuable when satellites cannot obtain good measurements, mainly in cloudy regions where, from a forecasting perspective, the need for accurate measurements is most vital. At first glance the applicability of GPS-IPW measurements over oceans is limited. But its deployment across island environments and on platforms such as oil rigs, buoys, and ships-representative of the oceanic environment in which they are embedded-has been proposed since they would undoubtedly yield significant benefits (Chadwell and Bock, 2001; Rocken *et al*., 2005). GPS-IPW complements other systems capable of measuring atmospheric moisture such as radiosondes, surface-based radiometers, satellite-based infrared and microwave sensors, research aircraft, and commercial aircraft, etc. However, it is not a substitute as it does not provide information about moisture profiles. Radiosondes provide tropospheric moisture profiles, but are expendable and because of the cost of these devices, they have limited spatial coverage

and are only launched two times per day-in some countries once per day. Surface-based microwave radiometers are capable of high temporal resolution but are costly, require frequent calibration, and their performance is adversely affected during the rain. Aircraft measurements are beginning to provide moisture observations using the Water Vapour Sounding Systems (WVSS) or Tropospheric Airborne Meteorological Data Reports (TAMDAR). However, these observations are limited to commercial operational locations and flight times, and are generally less continuous when compared to GPS-IPW observations. In fact, aircraft observations other than TAMDAR are generally limited to hub airport areas below 15 kft. The expense over each station is also very less. It also meets essential water vapour monitoring requirements not met by all other sensors, most significantly its ability to monitor water vapour under all weather conditions which is critical during potential severe weather events (United States Weather Research Program Prospectus Development Team Report; Emanuel *et al*., 1995). In addition, GPS-IPW accuracy of 1 to 2 mm (Deblonde *et al*., 2005) is equal to or better than integrated radiosonde moisture soundings (Gutman *et al*., 2005). Businger *et al*. (1996) and Puviarasan *et al*. (2010) have showed that GPS derived precipitable water (using sliding window technique) had good agreement with the independent radiosonde measurements over some stations. They have also found that for particular locations precipitable water vapour increases significantly before rainfall and decreases after the event.

Through Rapid Update Cycle (RUC) GPS-IPW data have been previously assimilated into mesoscale data assimilation and prediction system (Smith *et al.*, 2007). Benjamin *et al.*, 1998, Smith *et al*., 2000, Gutman and Benjamin, 2001 and Gutman *et al*., 2004 have described the results from GPS-IPW impact experiments with 60 km RUC (RUC60). Smith *et al*., 2007 have assessed the impact of GPS-IPW on moisture forecasts by analyzing several experimental versions of the Rapid Update Cycle. They have compared results from RUC60 forecasts initialized with and without GPS-IPW data over the 6-year period from 1999-2004. They show better forecasts with the GPS information. In NOAA Forecast Systems Laboratory (FSL), assimilation of GPS-IPW data has given improvement in short-range relative humidity forecasts, consistently (Smith *et al*., 2000). Kuo *et al*., 1993 have shown that on assimilation of GPS-IPW into a mesoscale model, it is possible to recover the vertical structure of the water vapour more accurately compared to the statistical retrieval based on climatology. They have also found improved short range precipitation forecasts after assimilation of GPS-IPW data.

In India earlier, Jade *et al*., 2005 have presented the results of integrated water vapour estimates from GPS data from continuously operating GPS stations established by C-MMACS (Centre for Mathematical Modelling and Computer Simulation) at Bangalore, Kodaikanal, Hanle and Shillong over the period 2001 to 2003. They showed realistic moisture with these GPS data. In another study by Balachandran and Geetha, 2010, analysis of hourly integrated precipitable water vapour data during northeast monsoon (NEM) season 2008, showed the signatures of NEM activity and the passage of tropical disturbances like cyclonic storms and depressions in the vicinity of the GPS observation site. The main objective of the present work is to investigate the impact of GPS Integrated Precipitable Water (GPS-IPW) on numerical weather prediction over Indian region.

3. Retrieval of precipitable water from Zenith wet delay

Total delay in the zenith direction (ZTD) is the sum of ZWD and ZHD, *i.e*.,

$$ZTD = ZWD + ZHD \quad (1)$$

ZHD is very sensitive to surface pressure and temperature and is calculated by the empirical formula:

$$ZHD = 0.00278 * P_S *[1+0.0026 * \cos(2\varphi) + 0.00000028 *Hs] \quad (2)$$

where, P_S = Surface Pressure in millibar,

H_S = Surface height above geoid in km and

φ = Latitude of the station.

Bevis, *et al*., 1994 have shown that the time-varying zenith wet delay observed at each GPS receiver in a network can be transformed into an estimate of the precipitable water overlying that receiver. This transformation is achieved by multiplying the zenith wet delay by a factor whose magnitude is a function of certain constants related to the refractivity of moist air and of the weighted mean temperature of the atmosphere. The mean temperature varies in space and time and must be estimated a priori in order to transform observed zenith wet delay into an estimate of precipitable water. So, according to Bevis *et al*., 1994 Zenith Wet Delay (ZWD) affecting a GPS receiver can be retrieved from the observations recorded by that receiver. It is based on the development of 'deterministic' least squares and Kalman filtering techniques. A particular GPS receiver simultaneously observes the signal delays from multiple radio sources that differ in their angles of elevation. Using

these techniques, it is now possible to retrieve the ZWD at each station in a continuously operating GPS network with good accuracy of less than 10 mm of long-term bias in equivalent excess path lengths, and less than 10 mm (RMS) of random noise.

The vertically integrated water vapour overlying a GPS receiver is proportional to the length of an equivalent column of liquid water, *i.e*., precipitable water (PW). It is expressed as

$$PW = \pi \times ZWD \tag{3}$$

where, the ZWD is given in units of length, and the dimensionless constant of proportionality π, which is given by

$$\pi = \frac{10^6}{\rho R_v [(k_3 / T_m) + k_2^{'}]} \tag{4}$$

(Askne and Nordius, 1987), where ρ is the density of liquid water, R_v is the specific gas constant for water vapour, and Tm is defined (Davis *et al*., 1985) as

$$T_m = \frac{\int (P_v / T)\, dz}{\int (P_v / T^2)\, dz} \tag{5}$$

where,

$$k_2^{'} = k_2 - mk_1 \tag{6}$$

and m is the ratio of the molar masses of water vapour and dry air. The physical constants k_1, k_2 and k_3 are widely used formula for atmospheric refractivity N (Smith and Weintraub 1953; Boudouris 1963):

$$N = k_1 \frac{P_d}{T} + k_2 \frac{P_v}{T} + k_3 \frac{P_{vd}}{T^2} \tag{7}$$

where, P_d and P_v are the partial pressures of dry air and water vapour, respectively and T is absolute temperature.

The values of the constants ρ, R_v, m are well determined, and their experimental uncertainties have no potential impact on the parameter π of equation (3). The uncertainties in π are derived from the uncertainties in the mean temperature of the atmosphere T_m and in the physical constants k_1, k_2 and k_3. For determination of the probable level of error in the parameter π, it is necessary to be able to specify values for the refractivity constants k_1, k_2 and k_3 and their associated uncertainties, for frequencies in the radio-microwave region of the spectrum. These constants have been determined by direct measurements made using microwave cavities (Boudouris 1963).

TABLE 1

Observations currently used in NCMRWF's data assimilation system

Observation type	Variables
Radiosonde	U, V T, q, P_S
Pibal winds	U, V
Wind profilers	U, V
Surface land observations	P_S
Surface ship and buoy observations	U, V, T, q, P_S
Conventional Aircraft observations (AIREP)	U, V, T
AMDAR Aircraft observations	U, V, T
ACARS Aircraft observations	U, V, T
GMS/MTSAT AMV (BUFR)	U, V, T
INSAT AMV	U, V, T
METEOSAT AMV (BUFR)	U, V, T
GOES (BUFR)	U, V, T
SSM/I	Surface wind speed
Scatterometer (QSCAT)	10 m U, V
AMSU-A radiance	Brightness temperature
AMSU-B radiance	Brightness temperature
HIRS radiance	Brightness temperature
SBUV ozone	Total ozone

4. Experimental setup

4.1. *Model used*

The present NCMRWF's Global Data Assimilation and Forecast System (GDAF) is based on NCEP (National Centre for Environmental Prediction) GFS (Global Forecast System). Gridpoint Statistical Interpolation (GSI) scheme for analysis is being used with the global model T254L64. The details of the above GSI are well documented by Rajagopal *et al*., 2007. The list of observations used in the assimilation system is tabulated in Table 1. The GSI analysis scheme uses three dimensional variational assimilation techniques. In this method a cost function is considered and the data is assimilated by minimizing the prescribed cost function through iteration. It uses the tangent linear and adjoint model for computation of gradients of cost function. The cost function consists of two terms; one for the contribution from the observations and the other term is the contribution from the background field. The distances

are scaled by the observation error covariance and by the background error covariance, respectively. Since the IPW measurements are not model analysis variable, for assimilation of IPW necessary interpolation and transformation from model analysis variables to IPW in the observation locations is required. An observation operator is used for this purpose. It does spatial interpolations (or spectral to physical space transformation) from the first guess to the location of the observations. The transformations are based on physical laws. For the present case, the observation operator is defined such that it first transforms from the analysis variables to IPW on a sigma-coordinate Gaussian grid and then interpolates these values to the observation locations.

The operator used for IPW is

$$P_w = \frac{p_s}{g} \sum_{\sigma=1}^{64} q_\sigma \Delta\sigma \tag{8}$$

where, q_σ is the specific humidity at the vertical level σ. The surface pressure p_s are obtained from the 6-hr forecast guess. The difference between the observed IPW and the transformed model first guess (Pw) denoted as "observational increments" or "innovations" are then obtained. The innovations so obtained are then converted in terms of model analysis parameter with the help of another operator which is the transpose of the integration in equation (8). The analysis is then obtained by adding the innovations to the model forecast (first guess) with weights that are determined based on the estimated statistical error covariances of the forecast and the observations.

4.2. *Period of study*

June is the month of monsoon onset over most of the Indian region. The onset dates vary from year to year. The monsoon winds approach the west coast of India from a westerly or south-westerly direction. The normal winds at the higher levels over Indian region in the month of June are mostly easterly. Along the monsoon trough which is extensive regions of low pressure, strong rising motion is observed. During this month the Indian region experiences dry to wet atmospheric conditions, with various monsoon related features getting settled over the place. So, the month of June 2008 was selected as the first study period with IPW data. This also gives the scope of extending the simulations for the entire monsoon period.

4.3. *Experiment*

The analysis and forecasts are carried out at horizontal triangular truncation of wave number 254 with 64 levels in the vertical. Global analysis are carried out four times (0000 UTC, 0600 UTC, 1200 UTC and 1800 UTC) a day with intermittent time scheme and with all the observations that are received at NCMRWF in +/- 3 hours time window. Model forecasts are integrated up to 168 hours. In the present study two sets of experiments were performed. In order to assess the impact of IPW over Indian region, GPS-IPW data of five Indian stations namely New Delhi, Kolkata, Guwahati, Mumbai and Chennai are assimilated and subsequent 168 hr forecasts are made through the NCMRWF's GFS for the month of June. The analysis and forecasts are also repeated for the entire period without the IPW data. The set of observations as shown in Table 1 and the model setup remains the same for both types of simulations. Henceforth, the experiments without IPW data will be termed as "CTRL" and those with IPW data will be termed as "IPW" / "EXP".

TABLE 2

RSRW generated and GPS estimated integrated precipitable Water (IPW) standard deviation over five stations for the month of June 2008 at 0000 and 1200 UTC

Stations	0000 UTC	0000 UTC	1200 UTC	1200 UTC
	RSRW	GPS	RSRW	GPS
Guwahati	14.20	4.89	12.98	4.33
Kolkata	7.94	5.33	6.31	5.78
Delhi	12.07	8.38	11.32	8.04
Chennai	7.02	3.31	8.85	5.18
Mumbai	14.01	9.35	-	10.11

TABLE 3

S_1 Scores for CTRL and IPW Geo-potential height at 850 and 250 hPa

	Indian region			
S_1 Score	850 hPa		250 hPa	
Days	CTRL	IPW	CTRL	IPW
1	35.2	35.3	35.1	35.2
2	38.2	37.6	37.8	37.8
3	41.9	41.8	40.2	40.1
4	45.1	41.5	42.4	42.1
5	47.4	46.9	44.3	44.0

5. Results and discussion

Right now the dataset used in this experiment is only over the five Indian stations. It is therefore is likely to have some impact mostly over India and surrounding regions. So the detailed study of the impact of GPS-IPW

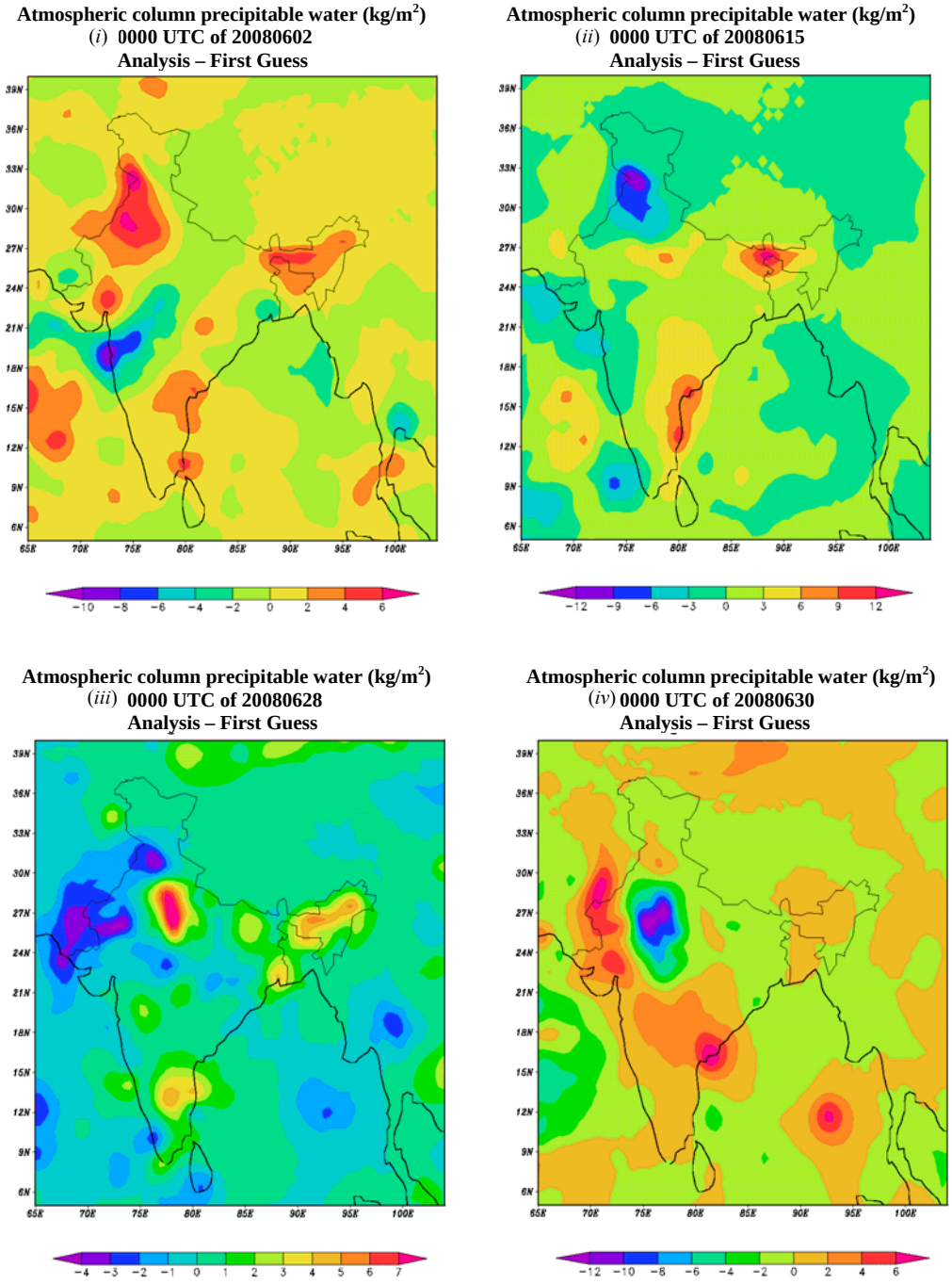

Figs. 1(*i-iv*). Difference between Analysis and First Guess Atmospheric Column Precipitable Water (kg/m^2) for IPW runs at 0000 UTC of (*i*) 2nd, (*ii*) 15th, (*iii*) 28th and (*iv*) 30th June, 2008

is examined with emphasis over India and the surrounding regions (10° S to 40° N, 40° to 100° E). The discussions are grouped into (*i*) Analysis *vs* Observations, (*ii*) Forecast *vs* Observation, (*iii*) Forecast *vs* Analysis and (*iv*) A synoptic case study. All the scores computed are averaged over the said region in space and time. 850 hPa pressure level is considered to represent lower troposphere, 500 hPa the mid-troposphere and 250/ 200 hPa the upper troposphere.

Prior to the discussions on the impact of the GPS-IPW on the analyses and simulated forecasts, comparison

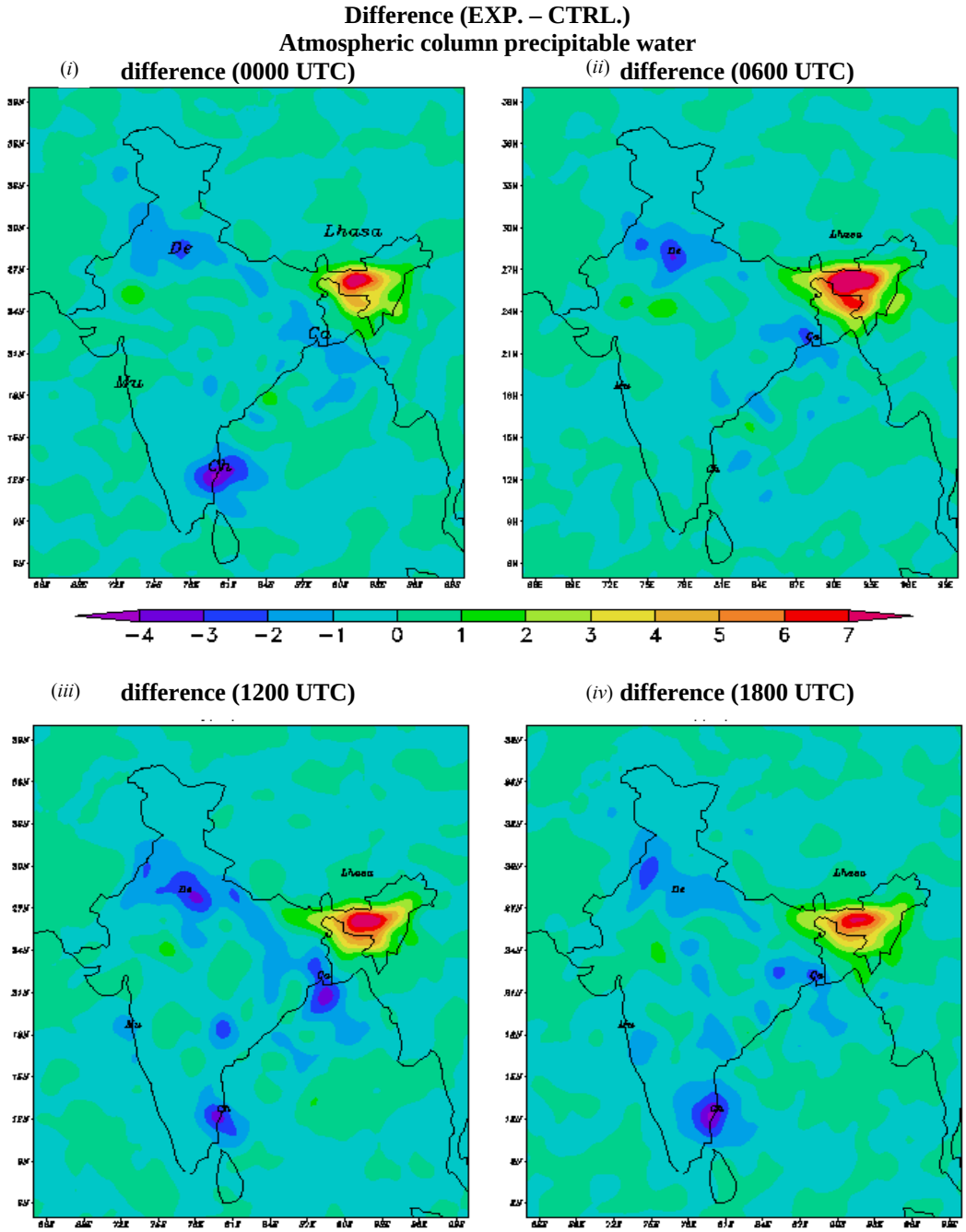

Figs. 2(i-iv). Difference between Mean Atmospheric Column Precipitable Water (kg/m^2) as obtained from control (CTRL) and experimental (EXP) analyses at (*i*) 0000, (*ii*) 0600, (*iii*) 1200 and (*iv*) 1800 UTC of June, 2008

has been made between the RSRW generated integrated precipitable water and GPS-IPW over the five Indian stations. Table 2 provides the standard deviation of integrated precipitable water measured by RSRW (Radio Sonde and Radio Wind) network and GPS at 0000 UTC and 1200 UTC over Guwahati, Kolkata, Delhi, Chennai and Mumbai. Due to non-availability of 1200UTC RSRW data over Mumbai, the corresponding part in Table 2 is left blank. From this table it could be inferred that the daily variation of the RSRW observed IPW (RSRW-IPW) is higher than the GPS estimated IPW (GPS-IPW). It is noted that the standard deviation of the RSRW-IPW is

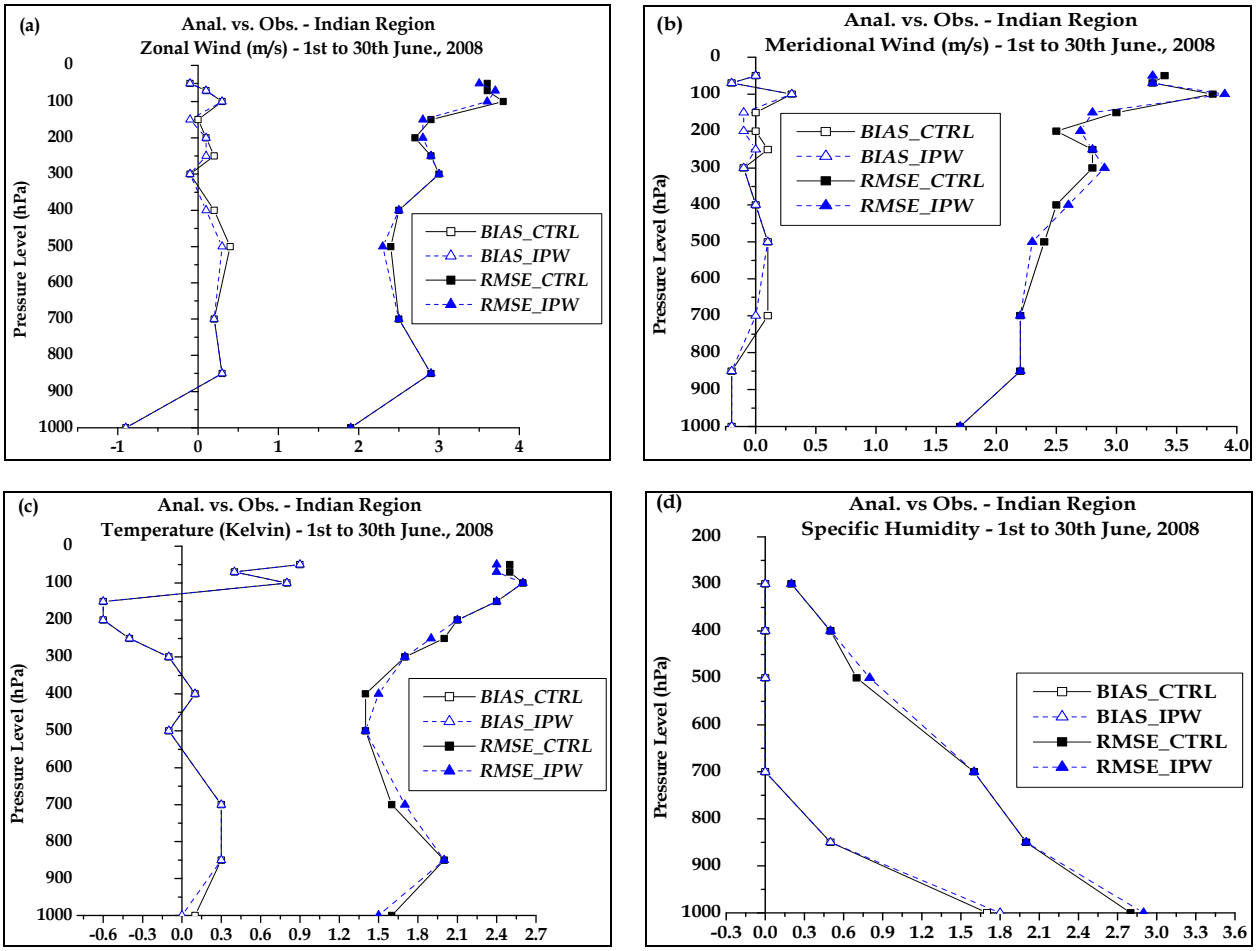

Figs. 3(a-d). Bias and root mean square error vertical profile of analysis from CTRL and IPW runs with respect to observations over Indian region for (a) zonal wind (m/s), (b) meridional wind (m/s), (c) temperature (Kelvin) and (d) specific humidity (gm/kg)

always higher over all the stations at both 0000 and 1200 UTC. Maxima of the RSRW recorded IPW is always higher compared to the GPS-IPW (figure not included).

Figs. 1(*i-iv*) represents the difference of atmospheric column precipitable water (kg/m^2) between the analysis using IPW data and the corresponding first guess used for the preparation of analysis. Four arbitrary dates are chosen, *viz*., [(*i*) 2nd, (*ii*) 15th, (*iii*) 28th & (*iv*) 30th June, 2008] starting from the beginning of the assimilation period till the end of the period of study. These figures are presented to highlight the impact over the analysis after the assimilation of IPW data. The assimilation of GPS-IPW data modifies the moisture profile over the stations. The modification and corresponding rectification of the moisture profile is propagated over the model domain through successive assimilation and forecasts, which leads to the difference visible in the atmospheric column precipitable water between the first guess and the corresponding analysis. Figs. 2(*i-iv*) shows the difference between mean atmospheric column precipitable water (kg/m^2) as obtained from control (CTRL) and experimental (EXP) analyses at (*i*) 0000, (*ii*) 0600, (*iii*) 1200 and (*iv*) 1800 UTC of June, 2008. It is found that over the five stations namely Guwahati, Kolkata, New Delhi, Mumbai and Chennai there is noticeable difference of mean analyzed atmospheric column precipitable water at (*i*) 0000, (*ii*) 0600, (*iii*) 1200 and (*iv*) 1800 UTC between the control and experimental runs, for June, 2008. Figs. 2(*i&ii*) reveal the modification of moisture profile due to IPW assimilation and the subsequent impact over the model initial conditions.

In the Analyses *vs* Observation study, Root Mean Square Error (RMSE) and bias of model analyses are computed against the radiosonde observation. RMSE over a region is computed from the squared error in the analysis with respect to the sounding data over the

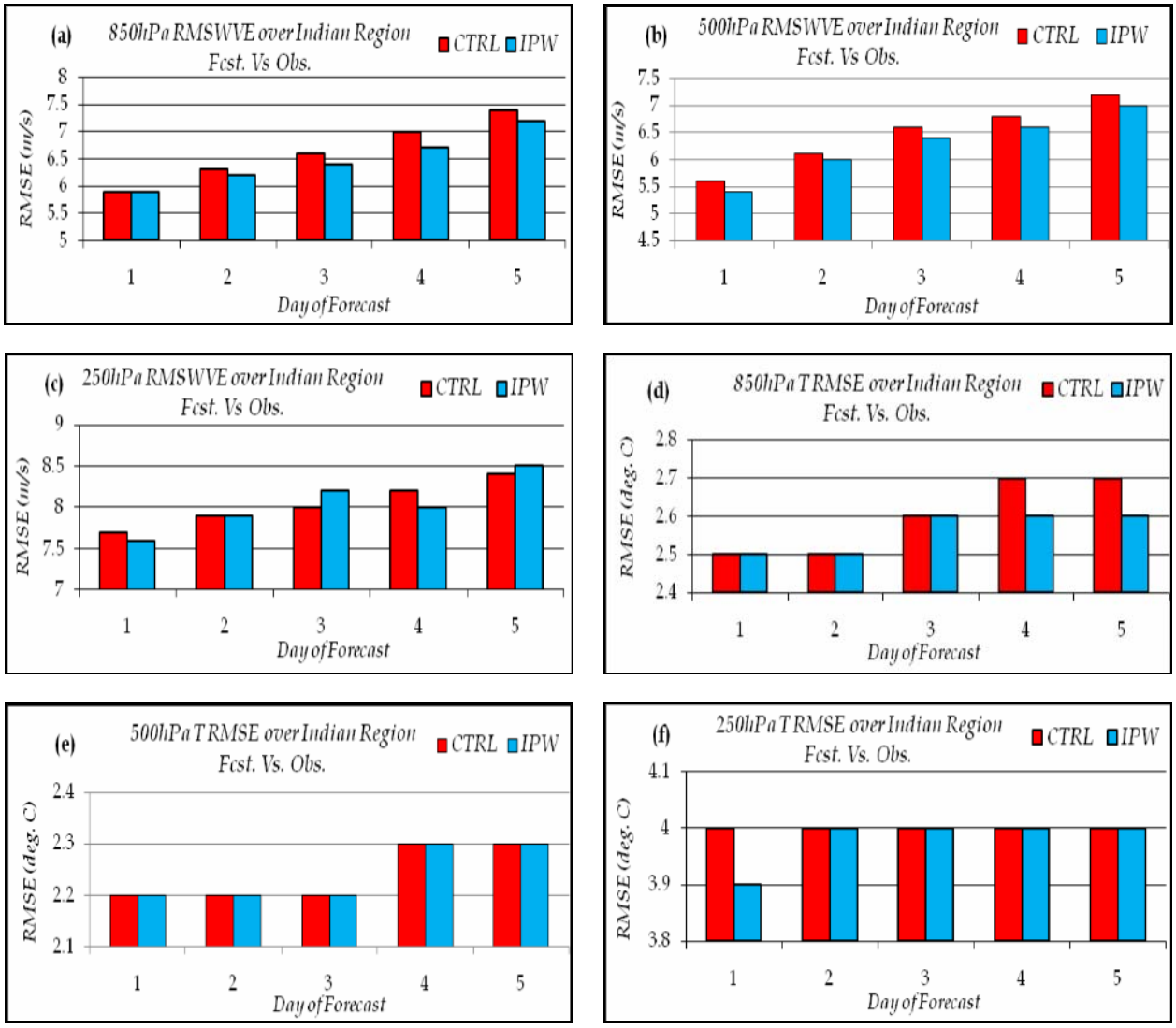

Figs. 4(a-f). Vector wind RMSE at (a) 850, (b) 500 & (c) 250 hPa pressure levels and temperature RMSE (0 °C) at (d) 850, (e) 500 & (f) 250 hPa pressure levels over Indian Region of T254L64 forecasts from CTRL and IPW runs with respect to observations

radiosonde stations in the said region and subsequent mean and square root over the entire region and for the entire period of study. Bias is the difference between the analyses and the observation, *i.e.*, the sounding data for the present study. Figs. 3(a-d) depicts the RMSE and bias over the Indian region for the analyses variables (a) zonal wind, (b) meridional wind, (c) temperature and (d) specific humidity with respect to the radiosonde observations. It is noted that for the layers above 750 hPa the zonal and meridional wind obtained from IPW analyses have less biases compared to that of CTRL analyses. The temperature and specific humidity have same biases for both experiments. Consistent improvement in the RMSE of the model analyses is not found in the IPW runs. In addition it is seen that there was no change found in the geo-potential RMSE and bias in the model analyses.

Impact over the model forecasts from the two different sets of simulations is also verified against the radiosonde observations. For comparison of Forecast *vs* Observation, forecast wind vector, temperature and geo-potential height RMSE are computed at 850, 500 and 250 hPa pressure levels. The forecast *vs* observation comparison has been restricted till forecast valid at day-5. The Figs. 4(a-f) presents the bar diagram plots for RMSE of wind vector Figs. 4(a-c) and RMSE of temperature Figs. 4(d-f) respectively. Forecasts from IPW simulations are found to have consistent lower wind vector RMSE at 850 and 500 hPa whereas at 250 hPa improvement in IPW

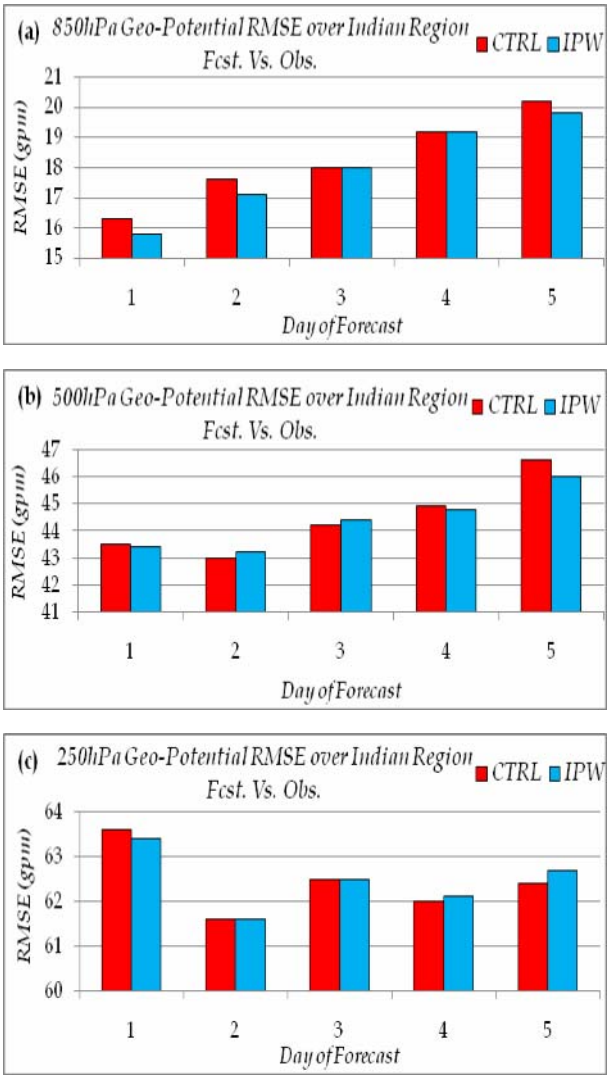

Figs. 5(a-c). Geo-potential height RMSE at (a) 850, (b) 500 & (c) 250 hPa pressure levels over Indian region of T254L64 forecasts from CTRL and IPW runs with respect to observations

runs are seen only for day-1 and day-4 forecasts. For temperature at 850 hPa, IPW forecasts are better compared to CTRL forecasts valid at day-4 & day-5. At 250 hPa, temperature RMSE for IPW runs is lower for day-1forecasts. For the other days the result remains the same for both the runs. At 500 hPa, temperature RMSE of both the runs is same for all the days of forecasts. Figs. 5 (a-c) depicts the geo-potential height RMSE histograms at 850 [Fig. 5(a)], 500 [Fig. 5(b)] and 250 hPa [Fig. 5(c)]. At 850 hPa, the IPW runs have lower geo-potential height forecast RMSE with respect to the analysis at day-1, 2 and 5. For day-3 and 4 the RMSE of both the simulated forecasts are same. At 500 hPa, positive impact is noticed for forecasts valid at day-1, 4 and 5 whereas at day-2 and day-3, the control forecasts have lower geo-potential

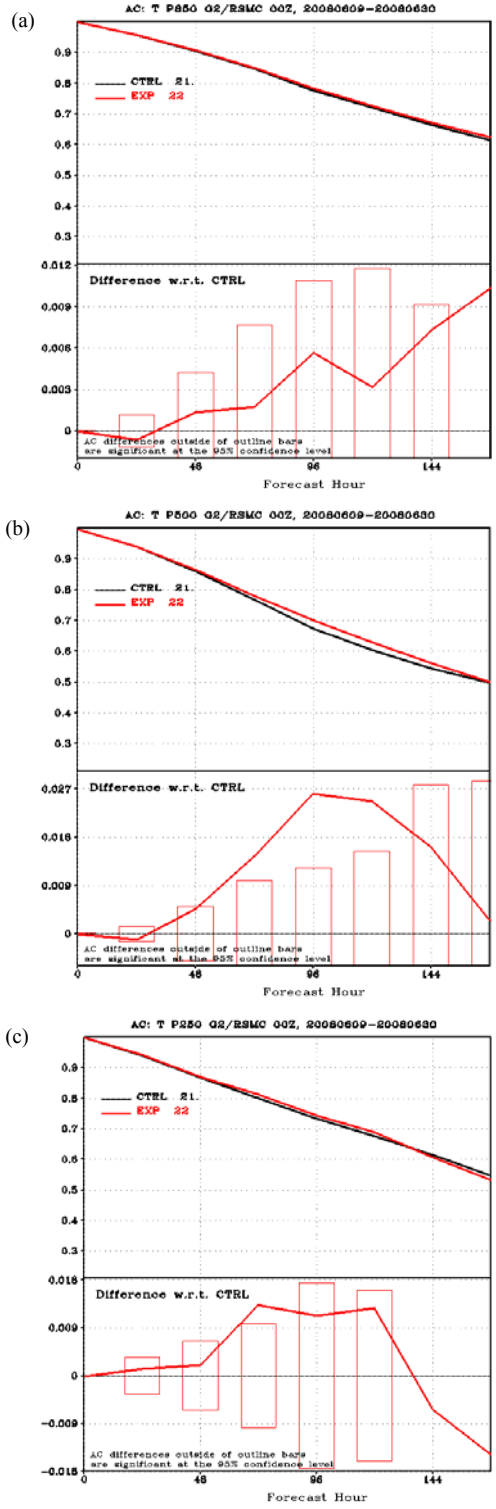

Figs. 6(a-c). Anomaly correlation over Indian region for Day-1 to Day-7 (upper part of the figures) and anomaly correlation difference of experimental simulations using IPW (EXP) w.r.t. control simulations (CTRL) along-with their statistical significance (lower part of the figures) for temperature at (a) 850 hPa, (b) 500 hPa and (c) 250 hPa pressure levels

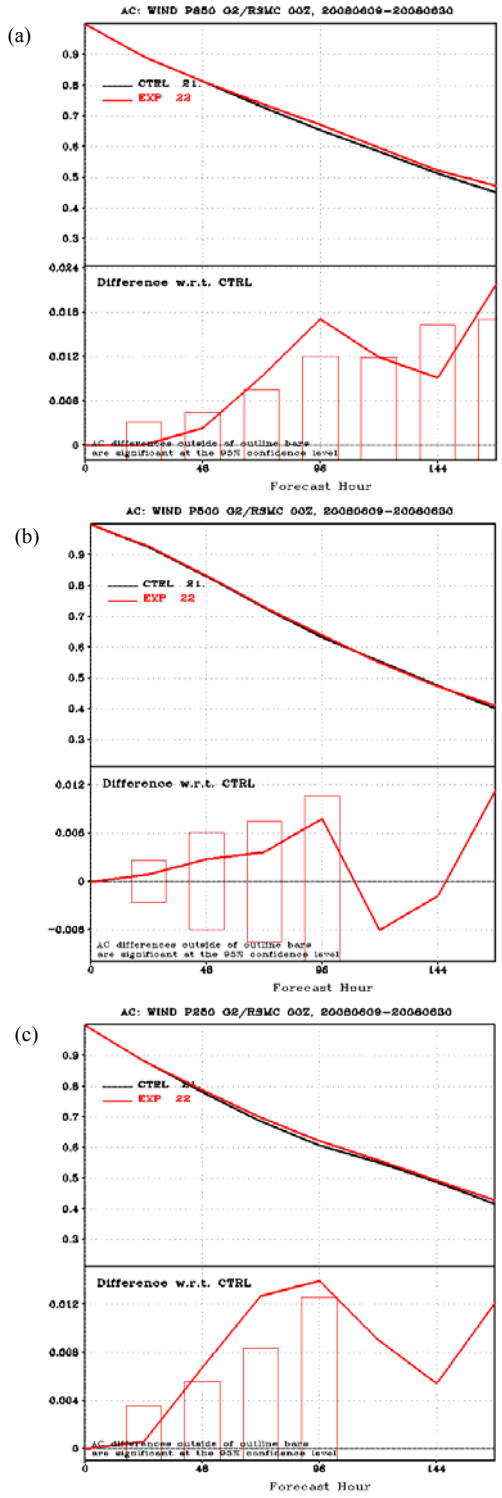

Figs. 7(a-c). Same as Fig. 6 but for vector wind

height RMSE. Over 250 hPa pressure level, IPW simulations have lower geo-potential height RMSE at day-1, whereas at day-4 and day-5, forecasts from control runs are at edge.

Performance of the model forecasts in terms of their respective analyses is also investigated. For the Forecast *vs* analyses study, comparisons were made in terms of Anomaly Correlation Coefficient, Pattern Correlation Coefficient, S_1 scores and Root Mean square Error. The anomaly co-relation coefficient is the co-relation between the observed and forecast anomalies. Pattern Correlation coefficient is the measure of the pattern similarity of the magnitude of the two variables – their covariance. S_1 scores represent how well the forecast gradients correspond to the observed gradients. It ranges from 0 to infinity. It is represented as

$$S_1 = 100 \frac{\sum_{i=1}^{n} (e_g)_i \cos \varphi_i}{\sum_{i=1}^{n} (G_L)_i \cos \varphi_i}$$

where,

$$e_g = \left[\left| \frac{\partial}{\partial x} (x_f - x_v) \right| + \left| \frac{\partial}{\partial y} (x_f - x_v) \right| \right]$$

$$G_L = \max \left[\left| \frac{\partial x_f}{\partial x} \right|, \left| \frac{\partial x_v}{\partial x} \right| \right] + \max \left[\left| \frac{\partial x_f}{\partial y} \right|, \left| \frac{\partial x_v}{\partial y} \right| \right]$$

where,

x_f = the forecast value of the parameter in question;

x_v = the corresponding verifying value (analyzed);

n = the number of grid points in the verification area;

cos φ_i = cosine of latitude of grid point i;

It is usually applied to geo-potential height or sea level pressure fields in meteorology. Because S_1 depends only on gradients, good scores can be achieved even when the forecast values are biased. For the present study S_1 scores were computed for the geo-potential height. S_1 score of geo-potential for day-1 to day-5 forecasts are tabulated in Table 3. S_1 score of IPW forecasts are showing marginal positive results over the CTRL runs for day-2 to day-5 at both 850 and 250 hPa pressure levels. On day-1 CTRL forecasts have lower S_1 score.

Figs. 6 (a-c) & 7 (a-c) depict the anomaly correlation over Indian Region for day-1 to day-7 (upper part of the figures) and anomaly correlation difference of experimental simulations using IPW (EXP) with respect to control simulations (CTRL) along-with their statistical significance (lower part of the figures) at (a) 850 hPa, (b) 500 hPa & (c) 250 hPa pressure levels for temperature

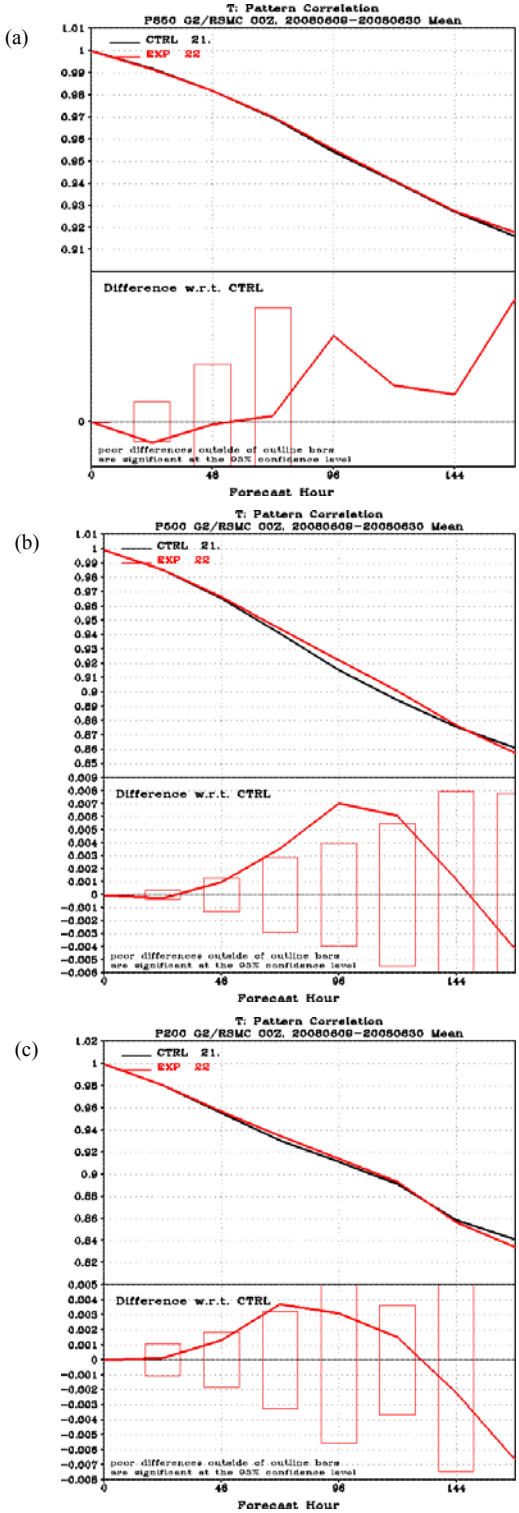

Figs. 8(a-c). Pattern correlation over Indian region for Day-1 to Day-7 (upper part of the figures) and pattern correlation difference of experimental simulations using IPW (EXP) w.r.t. control simulations (CTRL) along-with their statistical significance (lower part of the figures) for temperature at (a) 850 hPa, (b) 500 hPa and (c) 200 hPa pressure levels

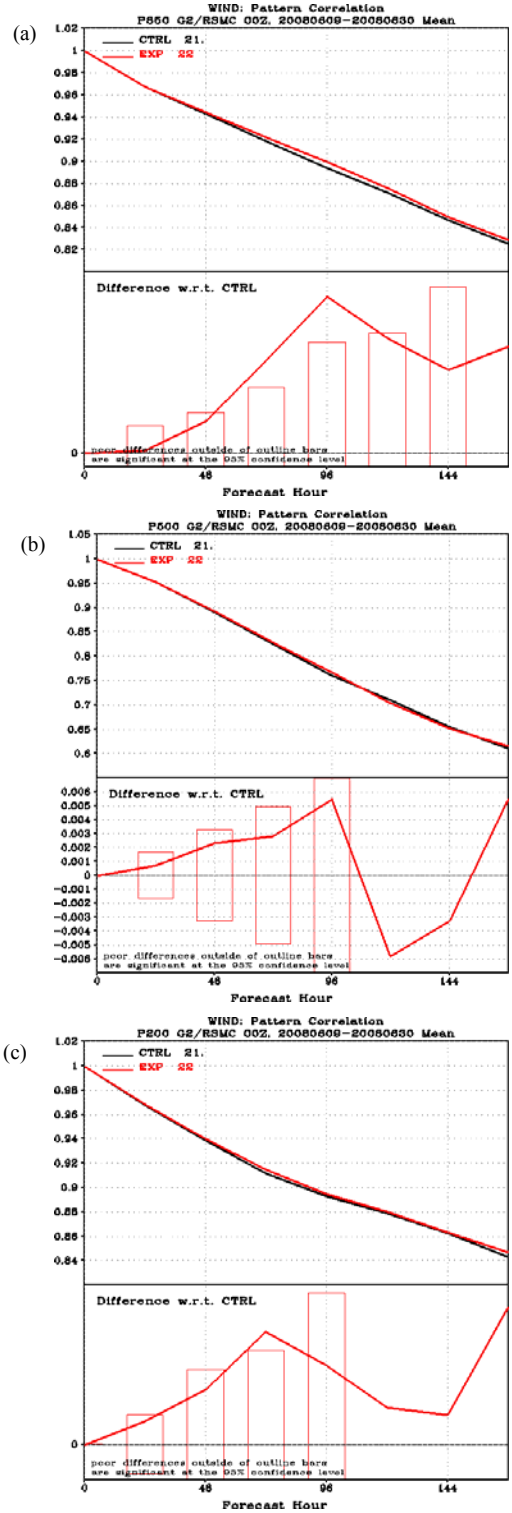

Figs. 9(a-c). Same as Fig. 8 but for vector wind

and vector wind, respectively. The difference values outside the histograms in the lower panel of the plots are statistically significant at 95% level of confidence. The CTRL here stands for the simulations without IPW

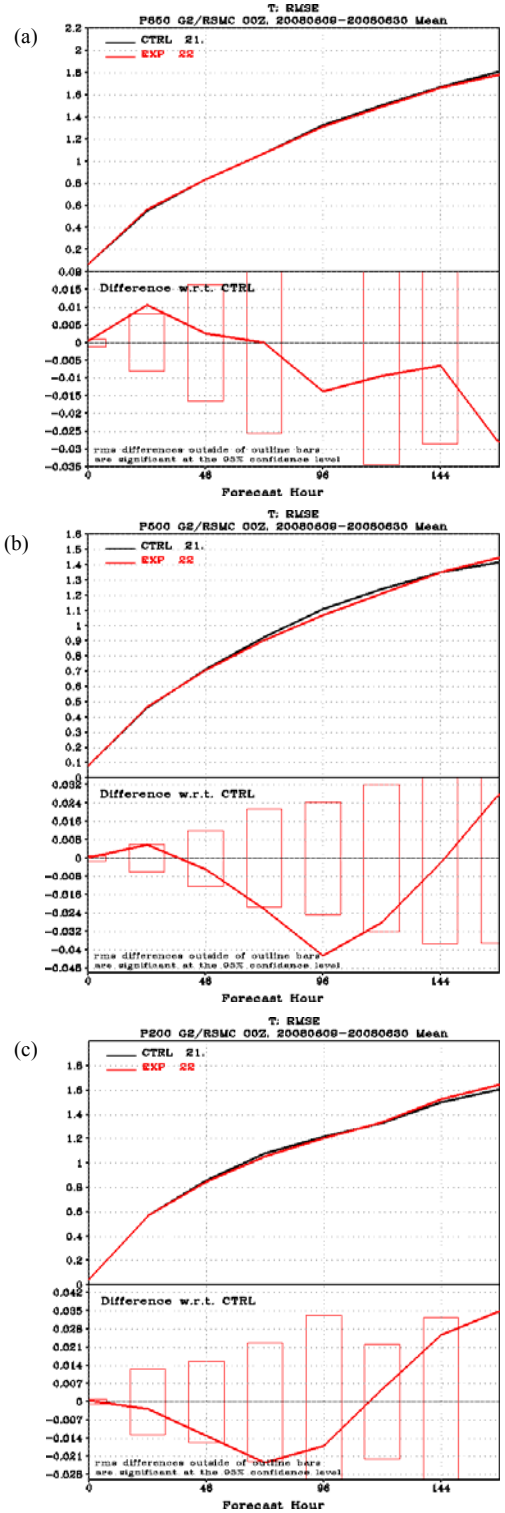

Figs. 10(a-c). Root Mean Square Error (RMSE) over Indian Region for Day-1 to Day-7 (upper part of the figures) and RMSE difference of experimental simulations using IPW (EXP) w.r.t control simulations (CTRL) along-with their statistical significance (lower part of the figures) for temperature at (a) 850 hPa, (b) 500 hPa & (c) 200 hPa pressure levels

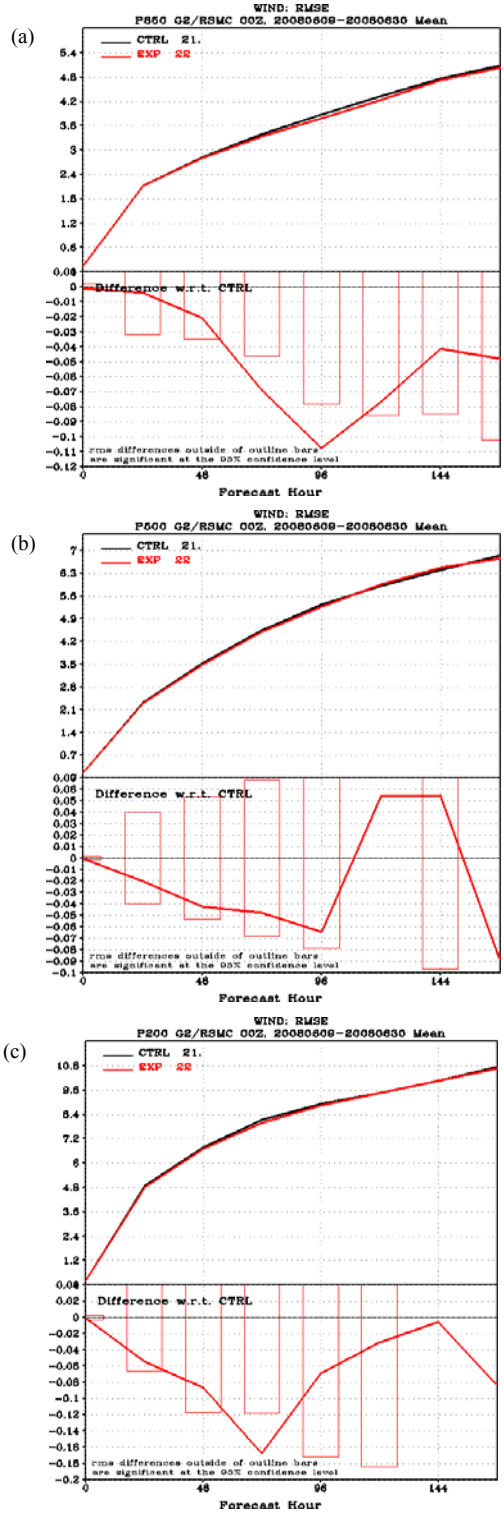

Figs. 11(a-c). Same as Fig. 10 but for vector wind

data and the EXP stands for the simulations with IPW assimilated initial conditions. For temperature anomaly correlation, significant positive impact of IPW is mainly

found at 500 hPa [Fig. 6(b)] for forecasts valid at day-3, day-4 and day-5. At 250 hPa [Fig. 6(c)], anomaly correlation of IPW forecasts valid at day-3 is significantly higher than that of the control forecasts. For vector wind, the significant impact is on day-3 & day-4 at 850 hPa]Fig. 7(a)] and on day-2, 3 and 4 at 250 hPa [Fig. 7(c)] pressure levels. For all other cases of forecast, the difference is either zero or not significant.

Pattern correlation is presented in the Figs. 8 (a-c) & 9 (a-c). The figures show the pattern correlation over Indian Region for day-1 till day-7 (upper part of the figures) and pattern correlation difference of experiments using IPW (EXP) with respect to control experiments (CTRL) along-with their statistical significance (lower part of the figures) at (a) 850 hPa, (b) 500 hPa and (c) 200 hPa pressure levels for temperature and vector wind, respectively. Significant impact of IPW on temperature pattern correlation is observed for day-3, 4 and 5 forecasts at 500 hPa [Fig. 8(b)] and day-3 forecasts at 200 hPa [Fig. 8(c)] pressure levels. For vector wind IPW forecasts valid for day-3 & 4 at 850 hPa [Fig. 9(a)] and for day-3 at 200 hPa [Fig. 9(c)] pressure level have significant higher pattern correlation. Pattern correlations of geo-potential height from IPW forecasts have significant higher value only for day-7 forecasts at 500 hPa and for day-3 forecasts at 200 hPa pressure levels. For all other cases of forecast, either there is no difference or it is insignificant.

In Figs. 10 (a-c) & 11(a-c) Root Mean Square Error (RMSE) over Indian Region for day-1 to day-7 (upper part of the figures) and RMSE difference of experimental simulations using IPW (EXP) with respect to control simulations (CTRL) along-with their statistical significance (lower part of the figures) at (a) 850 hPa, (b) 500 hPa & (c) 200 hPa pressure levels has been depicted for temperature and vector wind. Significant lower temperature RMSE for IPW forecasts is found for day-1 at 850 hPa [Fig. 10(a)] and day-4 at 500 hPa [Fig. 10(b)] pressure levels. For vector wind RMSE of IPW forecasts is significantly lower for day-3 & day-4 at 850 hPa [Fig. 11(a)] and for day-3 at 200 hPa [Fig. 11(c)] pressure levels. IPW forecasts valid for day-1 & 7 at 500 hPa and day-2 & 3 at 200 hPa (figures not included) have significantly lower geo-potential height RMSE. For all other cases of forecast, the difference is either zero or not significant.

5.1. *Monsoon in June, 2008*

In the year 2008, monsoon covered almost entire country except parts of West Rajasthan till 30th June. Rainfall activity over the country as a whole was above normal during the month. Central and northern parts of the country received excess rainfall. Among the chief synoptic features in the month of June, 2008, two depressions which formed over east central Arabian Sea (5-7 June, 2008) and North Bay of Bengal (16-18, June, 2008) were significant. On 17th June, 2008 a depression formed over the North Bay of Bengal which affected Gangetic West Bengal bringing heavy rainfall over the region. On this day, West Bengal received heavy rainfall of about 115-120 mm, highest for the month over the state. So for the present study, this day was selected as one of the days for rainfall comparisons between the two simulations. The above stated informations for June, 2008 were taken from Climate Diagnostics Bulletin of India (June, 2008) and Mazumdar *et al*., 2009.

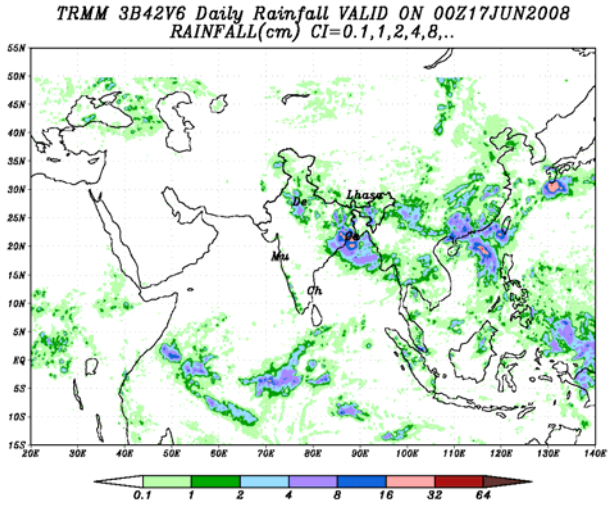

Fig. 12. TRMM 3B42-V6 accumulated rainfall (cm) valid at 0000 UTC of 17th June, 2008

5.2. *Rainfall*

Day-1, day-3 and day-5 rainfall forecasts valid at 0000 UTC of 17th June, 2008 as simulated by the CTRL and IPW runs are compared with that of TRMM-3B42V6 accumulated rainfall. TRMM rainfall is shown in Fig. 12. Figs. 13(a-f) depict the day-1, day-3 and day-5 rainfall forecasts of CTRL [Figs. 13(a-c)] and IPW [Figs. 13(d-f)] simulations. From Fig. 12 it is seen that the rainfall of about 16-32 cm. was observed over the coastal West Bengal and adjoining region. This rainfall amount is very well captured by day-1 forecast of IPW runs. CTRL run has suppressed the heavy intensity of the rainfall. Both CTRL and IPW simulations have shown decrease in the amount of rainfall in the subsequent forecasts valid at the same day. Reduction in the magnitude of rainfall over the coastal West Bengal and adjoining region is more in the CTRL runs compared to that of IPW runs.

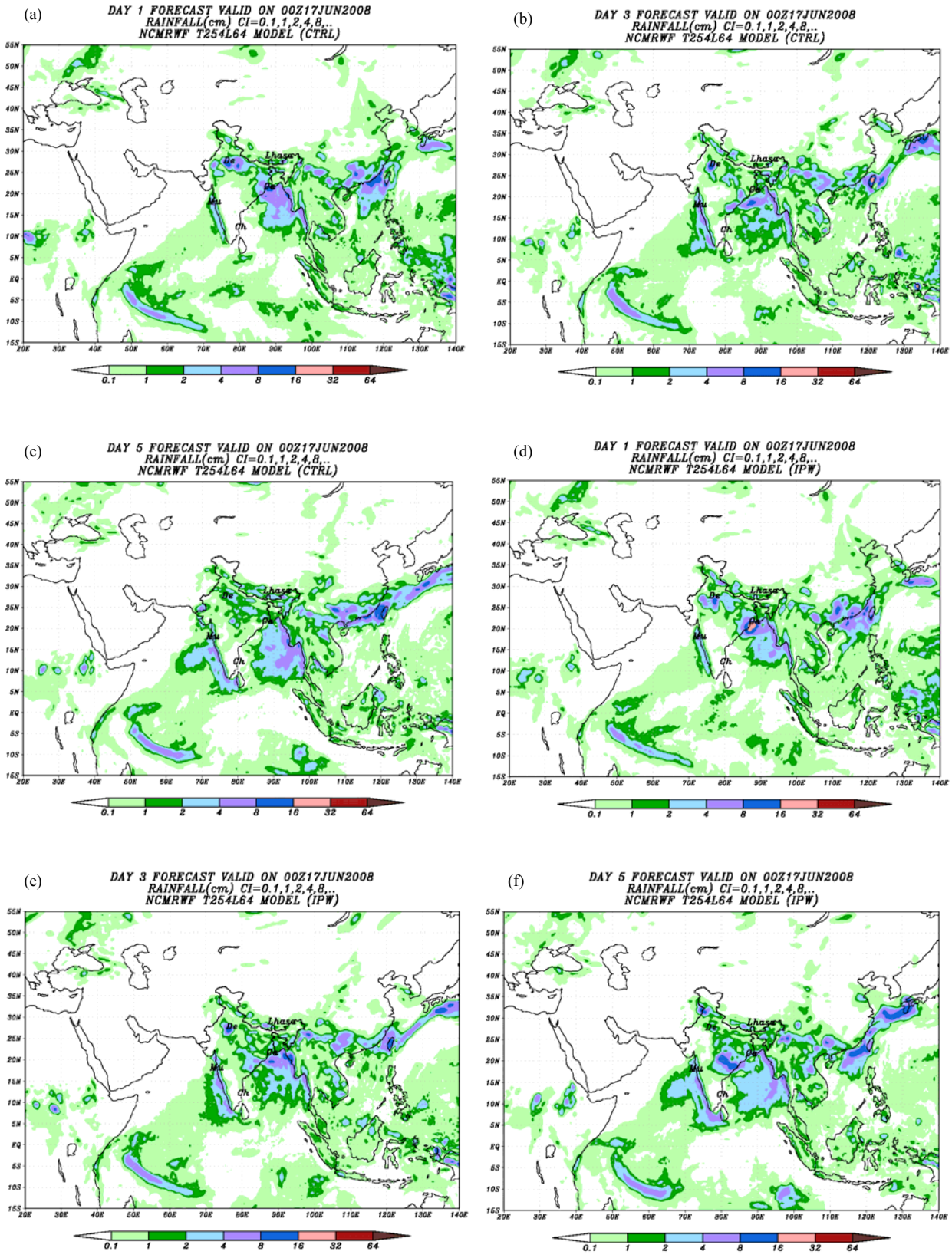

Figs. 13(a-f). Day-1, Day-3 and Day-5 Rainfall Forecasts valid at 0000 UTC of 17th June, 2008 of CTRL (a-c) and IPW (d-f)

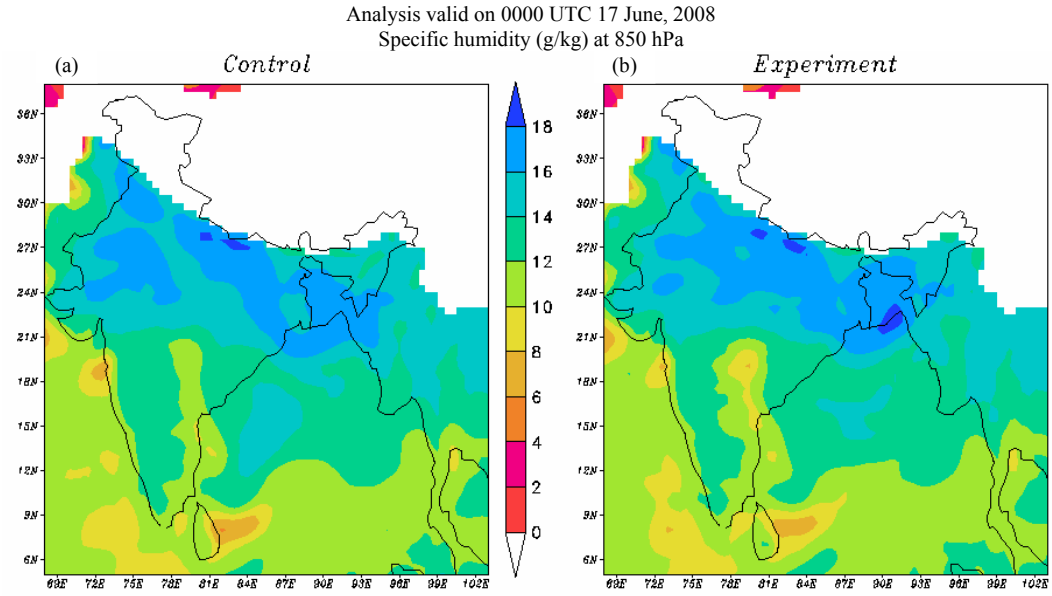

Figs. 14(a&b). Specific Humidity (g/kg) at 850 hPa for 0000 UTC of 17th June, 2008 as simulated by the (a) Control (CTRL) and (b) Experiment (IPW) runs

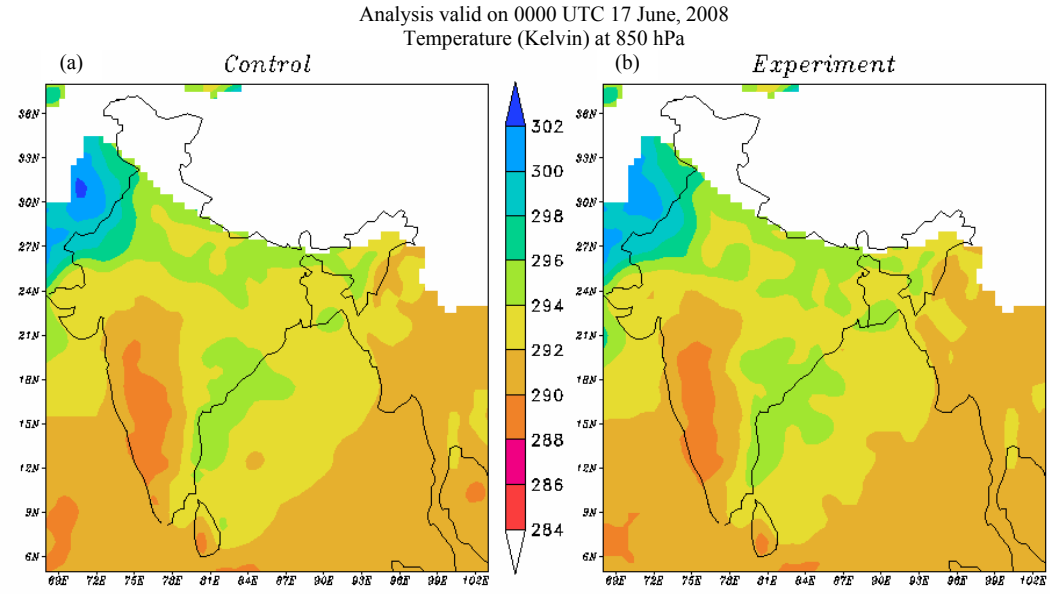

Figs. 15(a&b). Temperature (Kelvin) at 850 hPa for 0000 UTC of 17th June, 2008 as produced by the (a) Control (CTRL) & (b) Experiment (IPW) analyses

5.3. *Other parameters*

Figs. 14(a-b) depicts the specific humidity (gm/kg) and Figs. 15(a-b) represents the temperature (Kelvin) at 850 hPa of the CTRL and IPW analyses valid at 0000 UTC of 17th June, 2008. It is seen from the figures that both the parameters in IPW analyses have higher magnitude near coastal West Bengal. Higher rainfall as explained above could be the probable reason for the increased humidity in the simulated analyses using the IPW data. Also, with the precipitation, release of latent heat increases the air temperature, which explains the higher temperature values in the analysis using IPW data. The vertically integrated moisture transport at 0000 UTC of 17th June, 2008 does not show prominent change between the two analyses.

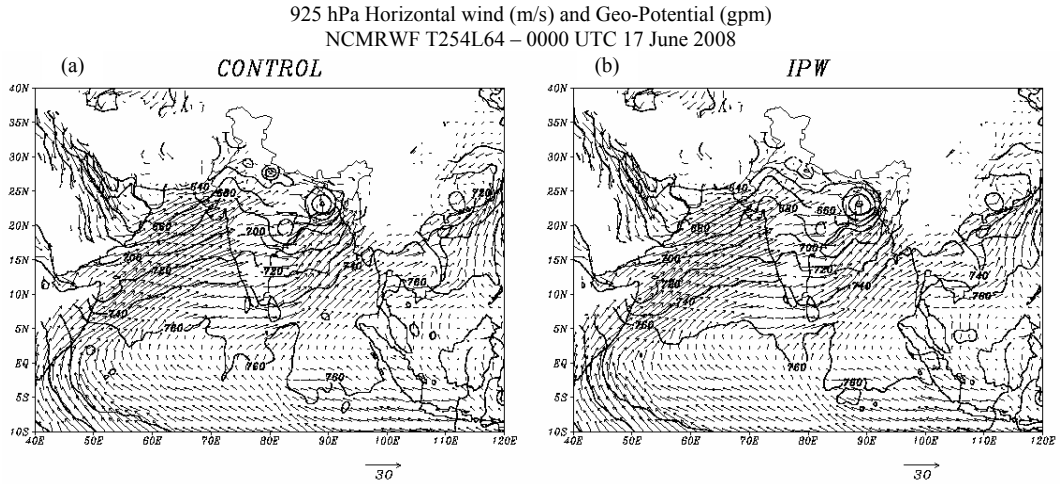

Figs. 16(a&b). 925 hPa horizontal wind (m/s) and geo-potential height (gpm) for 0000 UTC of 17th June, 2008 as produced by the (a) Control (CTRL) & (b) IPW analyses

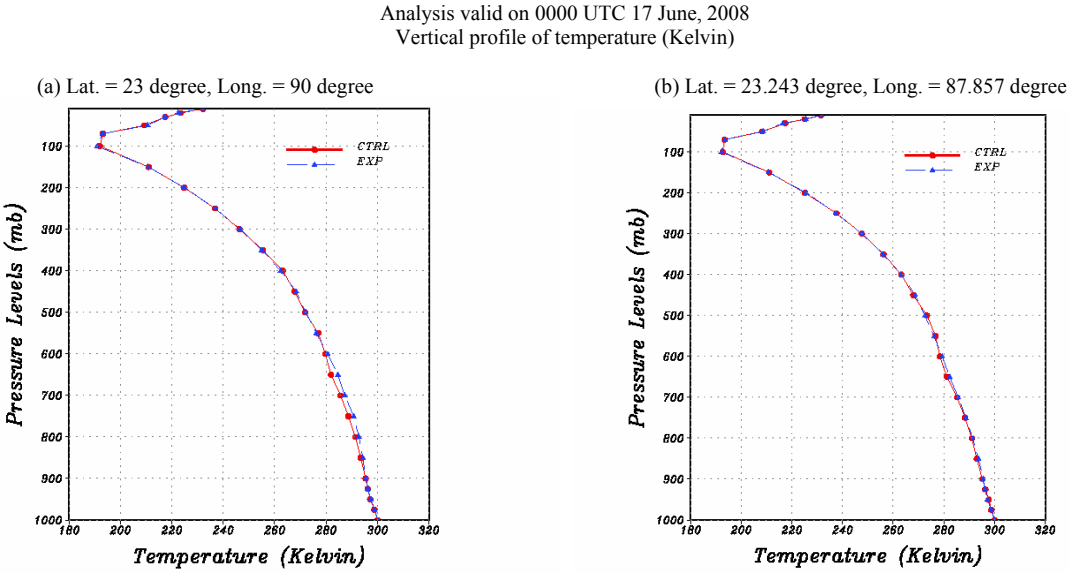

Figs. 17(a&b). Vertical profile of temperature (Kelvin) at (a) 23° N & 90° E (b) 23.243° N & 87.857° E, from control (CTRL) and experimental (EXP) analyses on 0000 UTC of 17th June, 2008

Figs. 16 (a-b) shows the horizontal wind (m/s) and geo-potential (gpm) at 925 hPa pressure level valid at 0000 UTC of 17th June, 2008 as produced by the CTRL and IPW analyses. The depression pattern near Gangetic West Bengal is similar for both the analyses. There is a small difference in the wind pattern around the depression.

Two arbitrary positions, one within the depression region very near to the centre and the other in the region surrounding the depression centre were chosen. The point 23° N latitude and 90° E longitude is located very near to the depression centre and the point 23.243° N latitude and 87.857° E longitude is situated in the region surrounding the depression centre. Figs. 17 (a&b) and 18(a&b) depict the vertical profile of temperature and specific humidity, respectively from the control and experimental analyses on 0000 UTC of 17th June, 2008 over the two locations. It is seen that within the lower troposphere (900-600 hPa), difference in temperature analyzed by two simulations [Figs. 17 (a&b)] is higher over the point located very near to the depression centre. Experimental analysis with IPW data has simulated higher temperature in the lower troposphere in the near vicinity of the depression centre. From the vertical profile of the specific humidity [Figs. 18(a&b)] it is found that near the depression centre experimental analysis has lower specific humidity in the

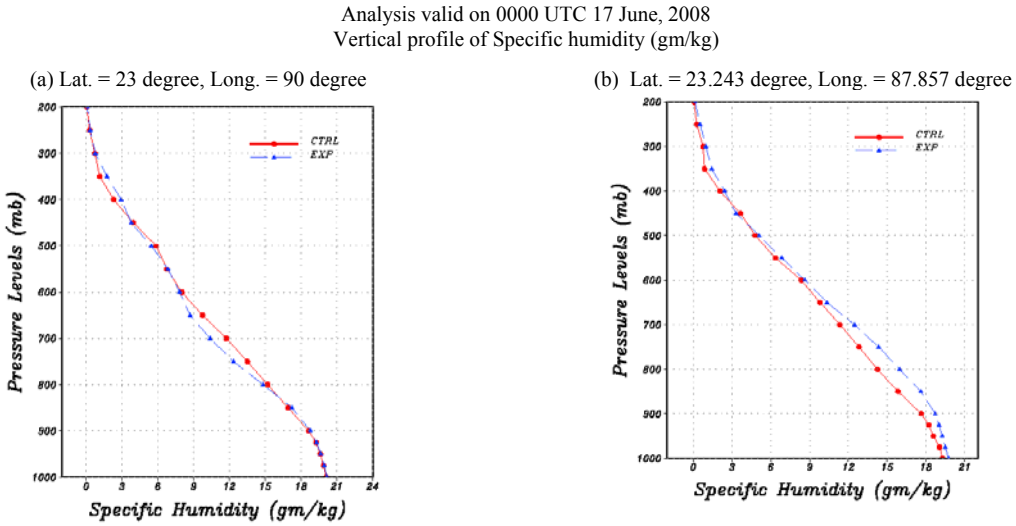

Figs. 18(a&b). Vertical profile of specific humidity (g/kg) at (a) 23° N & 90° E and (b) 23.243° N & 87.857° E, from control (CTRL) and experimental (EXP) analyses on 0000 UTC of 17th June, 2008

lower to middle troposphere. On the contrary, over the point located away from the depression centre, experimental analysis has higher specific humidity compared to the control analysis. The experimental analysis has dissipated more moisture near the depression centre [as also seen from the rainfall Figs. 13 (a-f)]. This has resulted in the decrease in humidity and increase in temperature due to latent heat release. Whereas in the region away from the depression centre, the situation reverses where due to less dissipation by the experimental simulation, there is larger moisture content and lowering of temperature in the experimental analysis compared to the control run.

6. Conclusions

This study examines the impact that GPS Integrated Precipitable Water has over various meteorological parameters. The study reveals that the assimilation of IPW data influences the analyses and corresponding forecasts of the weather model T254L64. This is the first attempt of assimilation of IPW data of the aforesaid five Indian stations in the global model and to study the corresponding impact over various meteorological parameters over Indian region. Though humidity is the primary parameter getting modified by IPW, indirect impact on other weather parameters are also in evitable. Change in humidity distribution will lead to change in the temperature which will eventually affect the pressure and wind field patterns. The results obtained in the present study are summarized below:

(*i*) The standard deviation of the RSRW-IPW is always higher over all the stations at both 0000 and 1200 UTC. Maxima of the RSRW recorded IPW is always higher compared to the GPS-IPW. RSRW-IPW is moister than GPS measured IPW.

(*ii*) When the analyses are compared with observations it is seen that for the layers above 850 hPa the zonal and meridional wind components for experimental analyses have less biases compared to that of CTRL analyses.

(*iii*) Comparing the forecasts with respect to the observations it is found that forecasts from experimental simulations have consistently lower wind vector RMSE at 850 and 500 hPa. For other variables like temperature and geo-potential height, the positive impact of IPW is not seen consistently over all the forecast days.

(*iv*) Forecasts *vs* analyses study shows that S_1 score of IPW forecasts are marginally better than CTRL runs for Day-2 to Day-5 at both 850 and 250 hPa pressure levels. On Day-1 CTRL forecasts have lower S_1 score. Positive impact of IPW assimilation is also seen from the anomaly and pattern correlations and RMSE. Correlation values are mostly higher and RMSE values are lower for experimental simulations. Statistically significant differences at 95% level of confidence with respect to the control values are also observed.

(*v*) The rainfall amount observed for 0000 UTC of 17th June, 2008 is very well captured by day-1 forecast of IPW runs. CTRL run has suppressed the heavy intensity of the rainfall.

(*vi*) Assimilation of IPW data has also shown the positive impact on the spatial pattern of various meteorological

parameters like specific humidity & temperature at 850 hPa and circulation patterns at 925 hPa analyses.

(*vii*) Difference in the vertical profile of temperature and specific humidity over the points located very close and away from the depression centre is also observed. Experimental analysis with IPW data has simulated higher temperature in the lower troposphere in the near vicinity of the depression centre. Near to the depression centre experimental analysis has lower specific humidity in the lower to middle troposphere. On the contrary, over the point located away from the depression centre, experimental analysis has higher specific humidity compared to the control analysis.

(*viii*) It is noted that the amount of data assimilated is less compared to the vastness of the domain. The difference in the results is solely due to the IPW data and is encouraging. By increasing the number of GPS-IPW stations over the Indian region and assimilation of their data in future, there is a scope of further improvements in the forecasts over the said region.

Acknowledgement

We gratefully acknowledge National Centre for Environmental Prediction (NCEP) for sharing the GSI code. We thank Director, NCMRWF for providing the necessary facilities to carry out this research work and for her encouragement and support. We also acknowledge Satellite Met. Division of India Meteorological Department, Delhi for providing the IPW data used in this experiment.

References

Askne, J. and Nordius, H., 1987, "Estimation of troposheric delay for microwaves from surface weather data", *Radio Sci*., **22**, 379-386.

Balachandran, S. and Geetha, B., 2010, "Signatures of northeast monsoon activity and passage of tropical cyclones in the integrated precipitable water vapour estimated through GPS technique", *Mausam*, **61**, 3, 349-360.

Benjamin, S. G., Smith, T. L., Schwartz, B. E., Gutman, S. I. and Kim, D., 1998, "Precipitation forecast sensitivity to GPS precipitable water observations combined with GOES using RUC-2", Preprints, 12th Conf. on Numerical Weather Prediction, Phoenix, AZ, *Amer. Meteor. Soc*., 249-252.

Bevis, M., Businger, S., Herring, T. A., Rocken, C., Anthes, R. A. and Ware, R. H., 1992, "GPS meteorology: Remote sensing of atmospheric water vapour using the Global Positioning System", *Journal of Geophysical Research*, **97**, 15,787-15,801.

Bevis, M., Businger S., Chiswell S., Herring T. A., Anthes R., Rocken C., and Ware R. H., 1994, GPS meteorology: Mapping zenith wet delays onto precipitable water", *Journal of Applied Meteorology*, **33**, 379-386.

Boudouris, G., 1963, "On the index of refraction of air, the absorption and dispersion of centimeter waves by gases", *Journal of Research of National Institute of Standards and Technology*, **67**D, 631-684.

Businger, S., Chiswell, S. R., Bevis, M., Duan, J., Anthes, R. A., Rocken, C., Ware, R. H., Exner, M., Hove, T. Van and Solheim, F. S., 1996 "The Promise of GPS in Atmospheric Monitoring" *Bulletin of American Meteorological Society*, **77**, 5-18.

Chadwell, C. D. and Bock, Y., 2001, "Direct estimation of absolute precipitable water in oceanic regions by GPS tracking of a coastal buoy", *Geophysical Research Letter*, **22**, 3701-3704.

Climate Diagnostics Bulletin of India: June 2008, Government of India, India Meteorological Department.

Davis, J. L., Herring, T. A., Shaprio, I. I., Rogers, A. E. and Elgered, G., 1985, "Geodesy by radio interferometry: Effects of atmospheric modelling errors on estimates of baseline length", *Radio Science*, **20**, 1593-1607.

Deblonde, G., Macpherson, S., Mireault, Y. and Héroux, P., 2005, "Evaluation of GPS precipitable water over Canada and the IGS network", *Journal of Applied Meteorology*, **44**, 153-166.

Duan, J., Bevis, M., Feng, P., Bock, Y., Chiswell, S. R., Businger, S., Rocken, C., Soldheim, F., Ware, R. H., Hering, T. A. and King R. W., 1996, "GPS meteorology: Direct estimation of the absolute value of precipitable water", *Journal of Applied Meteorology*, **35**, 830-838.

Emanuel, K. and co-authors, 1995, "United States Weather Research Program Prospectus Development Team Report", online report located at: http://www.esrl.noaa.gov/research/uswrp/PDT/PDT1.html.

Fang, P., Bevis, M., Bock, Y., Gutman, S. and Wolfe D., 1998, "GPS meteorology: Reducing systematic errors in geodetic estimates for zenith delay", *Geophysical Research Letters*, **25**, 3583-3586.

Gutman, S. I., Sahm, S. R., Benjamin, S. G., Schwartz, B. E., Holub, K. L., Stewart, J. Q. and Smith, T. L., 2004, "Rapid retrieval and assimilation of ground based GPS precipitable water observations at the NOAA Forecast Systems Laboratory: Impact on weather forecasts", *J. Meteor. Soc. Japan*, **82**, 351-360.

Gutman, S. I. and Benjamin, S. G., 2001, "The role of ground-based GPS meteorological observations in numerical weather prediction", *GPS Solutions*, **4**, 4, 16-24.

Gutman, S. I., Facundo, J. and Helms, D., 2005, "Quality control of radiosonde moisture observations", Preprints, Ninth Symposium on Integrated Observing and Assimilation Systems for Atmosphere, Oceans, and Land Surface (IOAS-AOLS), San Diego, CA, *Amer. Meteor. Soc*., CD-ROM, 11.7.

Hogg, D. C., Guiraud, F. O. and Decker, M. T., 1981, "Measurement of excess transmission length on earth-space paths", *Astron. Astrophys*., **95**, 304-307.

Jade, Sridevi, Vijayan M. S. M., Gaur, V. K., Prabhu Tushar, P., Sahu, S. C., 2005, "Estimates of precipitable water vapour from GPS data in the Indian subcontinent", *Int. J. Atm. Solar-Terrestrial Phys.*, **67**, 6, 623-635.

Kuo, Y. H., Guo, Y. R. and Westwater, E. R., 1993, "Assimilation of precipitable water measurements into a mesoscale numerical model", *Mon. Wea. Rev.*, **121**, 1215-1238.

Leick, A., 1990, "GPS Satellite Surveying", John Wiley, New York, p353.

Lijegren, J., Lesht, B., Hove, T. Van and Rocken, C., 1999, "A comparison of integrated water vapour from microwave radiometer, balloon-borne sounding system and Global Positioning System", Paper presented at the 9th Annual ARM Science Team Meeting, San Antonia, Texas, 22-26 March.

Liou, Y. A., Teng, Y. T., Hove, T. Van and Liljegren, J. C., 2001, "Comparison of precipitable water observations in the near tropics by GPS, microwave radiometer, and radiosondes", *Journal of Applied Meteorology*, **40**, 5-15.

MacDonald, A., Xie, Y. and Ware, R., 2002, "Diagnosis of three dimensional water vapour using slant observations from a GPS network", *Mon. Wea. Rev.*, **130**, 369-397.

Mazumdar, A. B., Khole, Medha and Devi, S. Sunitha, 2009, "Weather in India. Monsoon season (June to September, 2008)", *Mausam*, **60**, 3, 379-426.

Niell, A., 1996, "Global Mapping Functions for the Atmosphere Delay at Radio Wavelengths", *Journal of Geophysical Research*, **101**, 3227-3246.

Ohtani, R. and Naito, I., 2000, "Comparison of GPS-derived precipitable water vapours with radiosonde observations in Japan", *Journal of Geophysical Research*, **105**, 26,917-26,929.

Puviarasan, N., Giri, R. K. and Ranalkar, Manish, 2010: "Precipitable water vapour monitoring using ground based GPS system", *Mausam*, **61**, 2, 203-212.

Rajagopal, E. N., Gupta, Munmun Das, Mohandas, Saji, Prasad, V. S., George, John P., Iyengar, G. R. and Preveen Kumar, D., 2007, "Implementation of T254L64 Global Forecast System at NCMRWF", *NCMRWF Technical Report*, 1-42.

Rocken, C., Ware, R. H., Hove, T. Van, Solheim, F., Alber, C. and Johnson, J., 1993, "Sensing atmospheric water vapour with the Global Positioning System", *Geophysical Research Letters*, **20**, 2631-2634.

Rocken, C., Hove, T. Van and Ware, R., 1997, "Near real-time GPS sensing of atmospheric water vapour", *Geophysical Research Letters*, **24**, 3221-3224.

Rocken, C., Johnson, J., Hove, T. Van and Iwabuchi, T., 2005, "Atmospheric water vapour and geoid measurements in the open ocean with GPS", *Geophysical Research Letters*, **32**, 1-3.

Smith, E. K. and Weintraub, S., 1953, "The constants in the equation for atmospheric refractive index at radio frequencies", *Journal of Research of National Institute of Standards and Technology*, **50**, 39-41.

Smith, Tracy L., Stanley, G. Benjamin, Barry, Schwartz, E. and Seth, I. Gutman, 2000, "Using GPS-IPW in a 4-D data assimilation system", *Earth Planet. Space*, **52**, 921-926.

Smith, Tracy Lorraine, Stanley, G. Benjamin, Seth, I. Gutman and Susan, Sahm, 2007, "Short-Range Forecast Impact from Assimilation of GPS-IPW Observations into the Rapid Update Cycle", *Monthly Weather Review*, **135**, 2914-2930.

Solheim, F., Vivekanandan, J., Ware, R. and Rocken, C., 1999, "Propagation delays induced in GPS signals by dry air, water vapour, hydrometeors and other particulates", *Journal of Geophysical Research*, **104,** D8, 9663-9670.

Tregoning, P., Boers, R., O'Brien, D. and Hendy, M., 1998, "Accuracy of absolute precipitable water vapour estimates from GPS observations", *Journal of Geophysical Research*, **103**, 28,701- 28,710.

Ware, R. H., Alber, C., Rocken, C. and Solheim, F., 1997, "Sensing integrated water vapour along GPS ray paths", *Geophysical Research Letters*, **24**, 417-420.

Ware, R. H., Fulker, D. W., Stein, S. A., Anderson, D. N., Avery, S. K., Clark, R. D., Droegemeier, K. K., Kuettner, J. P., Minster, J. B., and Sorooshian, S., 2000, "SuomiNet: A real-time national GPS network for atmospheric research and education", *Bulletin of American Meteorological Society*, **81**, 677- 694..